



Phosphorus–nitrogen compounds. Part 23: Syntheses, structural investigations, biological activities, and DNA interactions of new N/O spirocyclophosphazenes

Nuran Asmafiliz^a, Zeynel Kılıç^{a,*}, Zeliha Hayvalı^a, Leyla Açık^b, Tuncer Hökelek^c, Hakan Dal^d, Yağmur Öner^b

^a Department of Chemistry, Ankara University, 06100 Ankara, Turkey

^b Department of Biology, Gazi University, 06500 Ankara, Turkey

^c Department of Physics, Hacettepe University, 06800 Ankara, Turkey

^d Department of Chemistry, Anadolu University, 26470 Eskişehir, Turkey

ARTICLE INFO

Article history:

Received 19 August 2011

Received in revised form 7 October 2011

Accepted 14 October 2011

Keywords:

N/O spirocyclophosphazenes

Syntheses

Spectroscopy

Crystal structure

DNA interactions

ABSTRACT

The Schiff base compounds (**1** and **2**) are synthesized by the condensation reactions of 2-furan-2-yl-methylamine with 2-hydroxy-3-methoxy- and 2-hydroxy-5-methoxy-benzaldehydes and reduced with NaBH₄ to give the new N/O-donor-type ligands (**3** and **4**). The monospirocyclophosphazenes containing 1,3,2-oxazaphosphorine rings (**5** and **6**) are prepared from the reactions of N₃P₃Cl₆ with **3** and **4**, respectively. The reactions of **5** and **6** with excess pyrrolidine, morpholine, and 1,4-dioxo-8-azaspiro [4,5] decane (DASD) produce tetrapyrrolidino (**5a** and **6a**), morpholino (**5b** and **6b**), and 1,4-dioxo-8-azaspiro [4,5] deca (**5c** and **6c**) spirocyclophosphazenes. The structural investigations of the compounds are examined by ¹H, ¹³C, ³¹P NMR, DEPT, HSQC, and HMBC techniques. The solid-state structures of **5**, **5a**, and **6** are determined using X-ray crystallography. The compounds **5a**, **5b**, **5c**, **6a**, **6b**, and **6c** are subjected to antimicrobial activity against six patojen bacteria and two yeast strains. In addition, interactions between these compounds and pBR322 plasmid DNA are presented by agarose gel electrophoresis.

© 2011 Elsevier B.V. All rights reserved.

1. Introduction

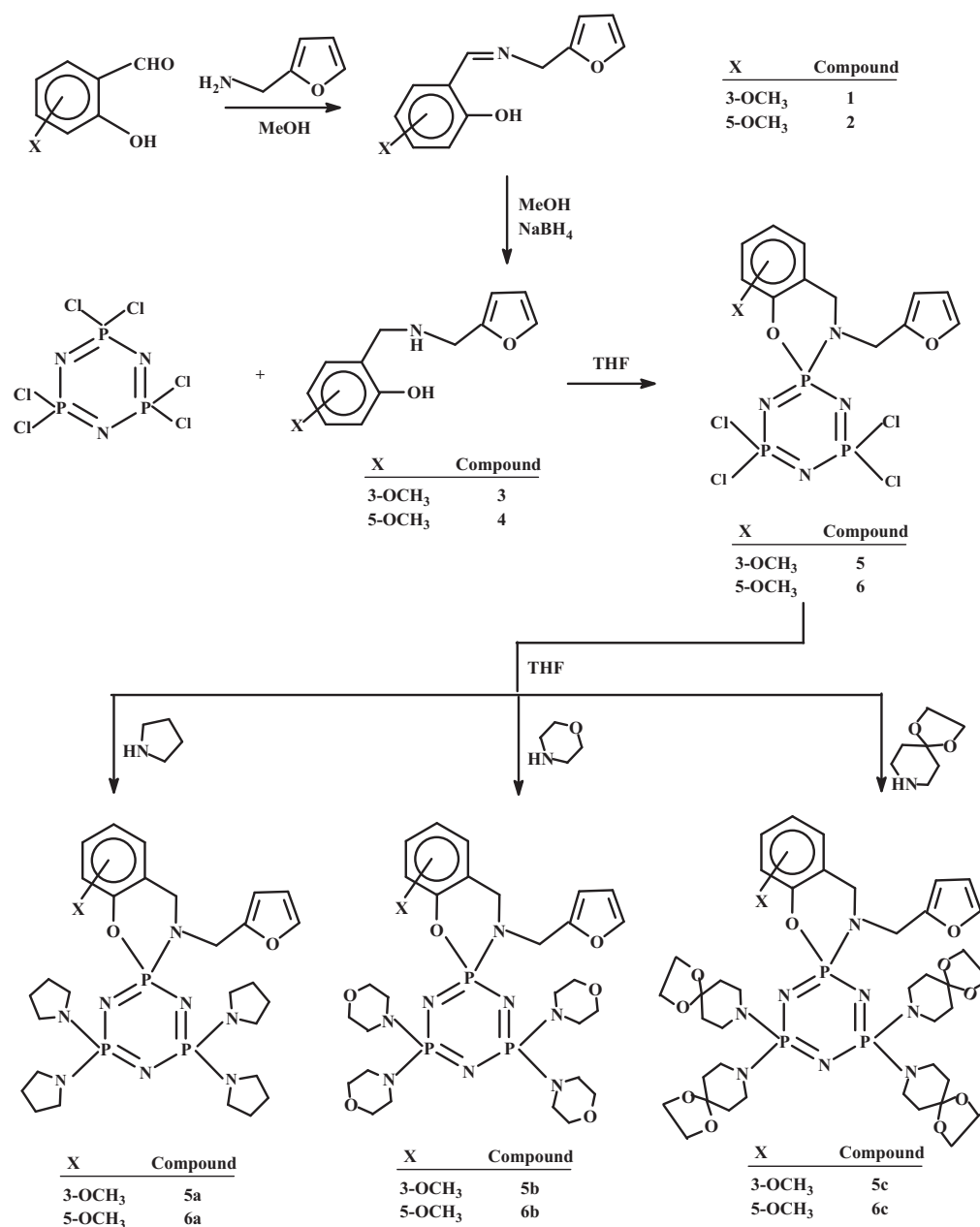
Organocyclophosphazenes (NPR₂)_n (*n* = 3, 4, ...), all of which contain phosphorus and nitrogen atoms bonded alternately, are borderline in inorganic and organic chemistry and an important family of inorganic ring systems [1–4]. A large number of the phosphazene derivatives have been prepared by nucleophilic substitution reactions on hexachlorocyclophosphazene, N₃P₃Cl₆, introducing easily a wide variety of different mono [5,6] and difunctional organic groups onto P atoms [7–9]. A scan of the literature shows that the involvement of bifunctional ligands with the cyclophosphazene ring is considerably limited to monofunctional reagents. The condensation reactions of bifunctional ligands with N₃P₃Cl₆ may lead to spiro, ansa, bino, dispiro, diansa, spiro-ansa, spiro-bino, and trispirocyclophosphazene derivatives [10–13]. On the other hand, the next oligomer octachlorocyclophosphazene, N₄P₄Cl₈, gives also similar products with bifunctional ligands [14–16].

As known, there are five possible reaction pathways for the reactions of N₃P₃Cl₆ with bidentate ligands: both functional groups of the ligand may replace with two chlorine atoms: (i) in cis

nongeminal route to give ansa derivatives and/or (ii) in geminal route to give spiro derivatives, (iii) the replacement of one chlorine atom with one of the two functional groups of the ligand to produce open-chain (dangling) compounds, (iv) intermolecular reactions between Cl atoms on two different phosphazene rings to form bridged (bino) phosphazene derivatives, and (v) intermolecular condensation reactions to give cycloliner or cyclomatrix polymers [17,18]. Moreover, the distribution of these phosphazene derivatives may depend on many factors, e.g. reaction time, solvent polarities, temperature, size of the phosphazene ring and the properties of the bifunctional ligands [19]. It has been observed that, when the reactions are carried out with N/O donor-type bidentate ligands and N₃P₃Cl₆, the major product is generally spiro derivative in tetrahydrofuran [20].

Recently, phosphazene derivatives have drawn considerable attention for the further design of highly selective anticancer agents [21] and antimicrobial [22] reagents. Aziridine-crown substituted cyclophosphazene derivatives cleave the DNA and halt the growth of cancer cells [23]. The Cu⁺² complex of fully-phenoxy-substituted star-branched cyclophosphazene derivative is also found to be active in the oxidative cleavage of DNA [24]. On the other hand, cyclophosphazenes have found industrial applications such as in the production of ionic liquids [25], liquid crystals [26], dendrimers having chiral ligands for asymmetric catalysis [27], flame retardants [28–30], advanced elastomers

* Corresponding author. Tel.: +90 3122126720/1043; fax: +90 3122232395.
E-mail address: zkilic@science.ankara.edu.tr (Z. Kılıç).



Scheme 1. The reaction pathway for the phosphazene derivatives.

[31,32], rechargeable batteries [33,34], and biomedical materials [35,36].

As a particular interest in our ongoing studies about N/O spirocyclic phosphazene derivatives, we report here in detail: (i) the synthesis of new N-(furan-2-yl-methyl)-3 and 5-methoxy-2-hydroxybenzylamines (**3** and **4**), (ii) the preparation of new tetrachloro (**5** and **6**), tetrapyrrolidino (**5a** and **6a**), tetramorpholino (**5b** and **6b**), and tetra(1,4-dioxo-8-azaspiro [4,5] deca) (**5c** and **6c**) monospirocyclotriphosphazenes (Scheme 1), (iii) investigations of antibacterial and antifungal activity of **5a**, **5b**, **5c**, **6a**, **6b**, and **6c**, and (iv) interactions between these compounds and pBR322 plasmid DNA examined by agarose gel electrophoresis. The determination of the structures of the compounds have been made using elemental analyses, mass spectrometry (MS), Fourier transform (FTIR), one-dimensional (1D) ¹H, ¹³C, and ³¹P NMR, distortionless enhancement by polarization transfer (DEPT), two-dimensional (2D) heteronuclear single quantum coherence (HSQC),

and heteronuclear multiple-bond correlation (HMBC) techniques. Moreover, the molecular and solid-state structures of **5**, **5a**, and **6** have been established by X-ray diffraction techniques.

2. Experimental

2.1. General methods

Hexachlorocyclotriphosphazatriene (Aldrich), 2-hydroxy-3-methoxy- and 2-hydroxy-5-methoxy-benzaldehydes (Aldrich), 2-furan-2-yl-methylamine (Acros Organics), pyrrolidine (Fluka), morpholine (Fluka), and 1,4-dioxo-8-azaspiro [4,5] decane (Fluka) were purchased and used without further purification. All reactions were monitored using thin-layer chromatography in different solvents and chromatographed using silica gel. All experiments were carried out in an argon atmosphere. The ¹H, ¹³C, and ³¹P NMR, DEPT, HSQC, and HMBC spectra were recorded on a Bruker

DPX FT-NMR (500 MHz) spectrometer (SiMe₄ as internal and 85% H₃PO₄ as external standards). The spectrometer was equipped with a 5 mm PABBO BB inverse-gradient probe. Standard Bruker pulse programs were used [37]. The IR spectra were recorded on a Mattson 1000 FTIR spectrometer in KBr disks and were reported in cm⁻¹ units. APIES mass spectrometric analyses were performed on an AGILENT 1100 MSD spectrometer. The melting points were measured on a Gallenkamp apparatus using a capillary tube. Antimicrobial susceptibility testing was performed by the agar-well diffusion method (Section S1 Supplementary Material). The DNA binding abilities were examined using agarose gel electrophoresis (Section S2 Supplementary Material).

2.2. Preparation of compounds

2-*[(E)-[(2-furanylmethyl)imino]methyl]-6-(methoxy)phenol* (**1**) was obtained from the reaction of 3-methoxy-2-hydroxy-benzaldehyde with 2-furan-2-yl-methylamine according to the methods reported in the literature [38].

2.2.1.

2-*[(E)-[(2-furanylmethyl)imino]methyl]-4-(methoxy)phenol* (**2**)

A solution of 5-methoxy-2-hydroxy-benzaldehyde (2.28 g, 15.00 mmol) in dry methanol (50 mL) was added to 1.45 g of 2-furan-2-yl-methylamine (15.00 mmol) in dry methanol (50 mL). The mixture was refluxed for 3 h and then the product was crystallized from methanol. Yield: 2.90 g (84%). mp: 77 °C. Anal. cal. for C₁₃H₁₃NO₃; C: 67.52; H: 5.67; N: 6.06. Found; C: 67.49; H: 5.63; N: 6.08%. FTIR (KBr, cm⁻¹): ν 3126 (O–H), 3091; 3065 (C–H arom.), 2967; 2880 (C–H aliph.).

2.2.2. 2-*[(2-Furanylmethyl)amino]methyl]-6-(methoxy)phenol* (**3**)

A solution of compound **1** (3.46 g, 15.00 mmol) in dry methanol (100 mL) was added to the excess sodium borohydride (2.28 g, 60.00 mmol). The crude product was extracted with dichloromethane (150 mL, three times). Yield: 0.86 g (86%). mp: 67 °C. Anal. cal. for C₁₃H₁₅NO₃; C: 66.94; H: 6.48; N: 6.00. Found; C: 67.13; H: 6.45; N: 5.94%. FTIR (KBr, cm⁻¹): ν 3301 (N–H), 3124 (O–H), 3106; 3046 (C–H arom.), 2996; 2935 (C–H aliph.).

2.2.3. 2-*[(2-Furanylmethyl)amino]methyl]-4-(methoxy)phenol* (**4**)

A solution of compound **2** (3.46 g, 15.00 mmol) in dry methanol (100 mL) was added to the excess sodium borohydride (2.28 g, 60.00 mmol). The crude product was extracted with dichloromethane (150 mL, three times). Yield: 0.90 g (90%). mp: 55 °C. Anal. cal. for C₁₃H₁₅NO₃; C: 66.94; H: 6.48; N: 6.00. Found; C: 66.86; H: 6.29; N: 6.17%. FTIR (KBr, cm⁻¹): ν 3289 (N–H), 3124 (O–H), 3091; 3065 (C–H arom.), 2960; 2890 (C–H aliph.).

2.2.4. 4',4',6',6'-Tetrachloro-3-(2-furanylmethyl)-8-(methoxy)-3H,4H-spiro{[1,3,2-benzoxazaphosphinine]-2,2'-[1,3,5,2,4,6]triazatriphosphinine} (**5**)

A solution of **3** (1.00 g, 4.29 mmol) in THF (150 mL) and triethylamine (1.21 mL) was added to a stirred solution of N₃P₃Cl₆ (1.49 g, 4.29 mmol) in THF (50 mL) at room temperature. The mixture was stirred for 25 h and the precipitated triethylaminehydrochloride was filtered off. The solvent was evaporated and the product purified by column chromatography with benzene. The powdery product was crystallized from acetonitrile. Yield: 1.71 g (78%). mp: 125 °C. Anal. cal. for C₁₃H₁₃N₄O₃P₃Cl₄; C: 30.74; H: 2.58; N: 11.03. Found; C: 30.70; H: 2.45; N: 11.07%. FTIR (KBr, cm⁻¹): ν 3092; 3076

(C–H arom.), 2972; 2875 (C–H aliph.), 1236; 1174 (P=N), 564; 527 (PCL). APIES-MS (based on ³⁵Cl, Ir %): *m/z* = 507 ([MH]⁺, 26%).

2.2.5. 4',4',6',6'-Tetrachloro-3-(2-furanylmethyl)-6-(methoxy)-3H,4H-spiro{[1,3,2-benzoxazaphosphinine]-2,2'-[1,3,5,2,4,6]triazatriphosphinine} (**6**)

The work-up procedure was similar to that of compound **5**, using **4** (1.70 g, 7.30 mmol), N₃P₃Cl₆ (2.54 g, 7.30 mmol) and triethylamine (2.05 mL). Yield: 2.68 g (72%). mp: 96 °C. Anal. cal. for C₁₃H₁₃N₄O₃P₃Cl₄; C: 30.74; H: 2.58; N: 11.03. Found; C: 30.80; H: 2.62; N: 10.90%. FTIR (KBr, cm⁻¹): ν 3117; 3074 (C–H arom.), 2934; 2839 (C–H aliph.), 1242; 1186 (P=N), 581; 519 (PCL). APIES-MS (based on ³⁵Cl, Ir %): *m/z* = 507 ([MH]⁺, 90%).

2.2.6. 4',4',6',6'-Tetra(1-pyrrolidinyl)-3-(2-furanylmethyl)-8-(methoxy)-3H,4H-spiro{[1,3,2-benzoxazaphosphinine]-2,2'-[1,3,5,2,4,6]triazatriphosphinine} (**5a**)

A solution of compound **5** (0.90 g, 1.77 mmol) and triethylamine (1.00 mL) in dry THF (150 mL) was added slowly to a solution of pyrrolidine (1.74 mL, 21.00 mmol) with stirring and refluxing for 30 h. The oily product was purified by column chromatography using benzene-THF (2:1) as an eluent and was crystallized from acetonitrile. Yield: 0.67 g (59%). mp: 113 °C. Anal. cal. for C₂₉H₄₅N₈O₃P₃; C: 53.87; H: 7.01; N: 17.33. Found; C: 53.97; H: 6.86; N: 17.20%. FTIR (KBr, cm⁻¹): ν 3098; 3058 (C–H arom.), 2964; 2852 (C–H aliph.), 1224; 1199 (P=N). APIES-MS (based on ³⁵Cl, Ir %): *m/z* = 647 ([M]⁺, 100%).

2.2.7. 4',4',6',6'-Tetra(1-pyrrolidinyl)-3-(2-furanylmethyl)-6-(methoxy)-3H,4H-spiro{[1,3,2-benzoxazaphosphinine]-2,2'-[1,3,5,2,4,6]triazatriphosphinine} (**6a**)

The work-up procedure was similar to that of compound **5a**, using **6** (1.08 g, 2.13 mmol), pyrrolidine (2.09 mL, 26.00 mmol) and triethylamine (1.20 mL). Yield: 0.85 g (62%). mp: 145 °C. Anal. cal. for C₂₉H₄₅N₈O₃P₃; C: 53.87; H: 7.01; N: 17.33. Found; C: 53.97; H: 6.86; N: 17.18%. FTIR (KBr, cm⁻¹): ν 3097; 3056 (C–H arom.), 2964; 2859 (C–H aliph.), 1220; 1186 (P=N). APIES-MS (based on ³⁵Cl, Ir %): *m/z* = 647 ([M]⁺, 100%).

2.2.8. 4',4',6',6'-Tetra(4-morpholinyl)-3-(2-furanylmethyl)-8-(methoxy)-3H,4H-spiro{[1,3,2-benzoxazaphosphinine]-2,2'-[1,3,5,2,4,6]triazatriphosphinine} (**5b**)

To a THF (75 mL) solution of **5** (1.00 g, 1.96 mmol) and triethylamine (1.10 mL) was added 2.05 mL of morpholine (24.00 mmol) in THF (75 mL) and the mixture was refluxed for 27 h. The solvent was evaporated and the crude product was purified by column chromatography with benzene-THF (1:1). Yield: 0.81 g (58%). mp: 160 °C. Anal. cal. for C₂₉H₄₅N₈O₇P₃; C: 49.01; H: 6.34; N: 15.77. Found; C: 48.88; H: 6.13; N: 15.73%. FTIR (KBr, cm⁻¹): ν 3091; 3071 (C–H arom.), 2960; 2842 (C–H aliph.), 1255; 1185 (P=N). APIES-MS (based on ³⁵Cl, Ir %): *m/z* = 711 ([M]⁺, 100%).

2.2.9. 4',4',6',6'-Tetra(4-morpholinyl)-3-(2-furanylmethyl)-6-(methoxy)-3H,4H-spiro{[1,3,2-benzoxazaphosphinine]-2,2'-[1,3,5,2,4,6]triazatriphosphinine} (**6b**)

The work-up procedure was similar to that of compound **5b**, using **6** (1.20 g, 2.36 mmol), morpholine (2.47 mL, 28.00 mmol) and triethylamine (1.33 mL). Yield: 0.90 g (54%). mp: 157 °C. Anal. cal. for C₂₉H₄₅N₈O₇P₃; C: 49.01; H: 6.34; N: 15.77. Found; C: 49.31; H: 6.30; N: 15.56%. FTIR (KBr, cm⁻¹): ν 3093; 3075 (C–H arom.), 2962;

2848 (C–H aliph.), 1255; 1187 (P=N). APIES-MS (based on ^{35}Cl , Ir %): $m/z = 711$ ($[\text{M}]^+$, 100%).

2.2.10. 4',4',6',6'-Tetra(1,4,7-dioxazonan-7-yl)-3-(2-furanylmethyl)-8-(methoxy)-3H,4H-spiro{[1,3,2-benzoxazaphosphinine]-2,2'-[1,3,5,2,4,6]triazatriphosphinine} (**5c**)

The mixture of **5** (0.62 g, 1.22 mmol), triethylamine (0.69 mL) and DASD (1.88 mL, 14.64 mmol) in THF (150 mL) was refluxed for 30 h. The product was purified by column chromatography with benzene-THF (1:1). Yield: 0.69 g (60%). mp: 181–183 °C. Anal. cal. for $\text{C}_{41}\text{H}_{61}\text{N}_8\text{O}_{11}\text{P}_3$; C: 52.67; H: 6.58; N: 11.99. Found; C: 52.47; H: 6.53; N: 11.78%. FTIR (KBr, cm^{-1}): ν 3071; 3056 (C–H arom.), 2954; 2844 (C–H aliph.), 1205; 1156 (P=N). APIES-MS (based on ^{35}Cl , Ir %): $m/z = 935$ ($[\text{M}]^+$, 100%).

2.2.11. 4',4',6',6'-Tetra(1,4,7-dioxazonan-7-yl)-3-(2-furanylmethyl)-6-(methoxy)-3H,4H-spiro{[1,3,2-benzoxazaphosphinine]-2,2'-[1,3,5,2,4,6]triazatriphosphinine} (**6c**)

The work-up procedure was similar to that of compound **5c**, using **6** (0.75 g, 1.48 mmol), DASD (2.27 mL, 18.00 mmol) and triethylamine (0.83 mL). Yield: 0.87 g (63%). mp: 168 °C. Anal. cal. for $\text{C}_{41}\text{H}_{61}\text{N}_8\text{O}_{11}\text{P}_3$; C: 52.67; H: 6.58; N: 11.99. Found; C: 52.44; H: 6.53; N: 12.03%. FTIR (KBr, cm^{-1}): ν 3091; 3075 (C–H arom.), 2954; 2846 (C–H aliph.), 1215; 1174 (P=N). APIES-MS (based on ^{35}Cl , Ir %): $m/z = 935$ ($[\text{M}]^+$, 100%).

2.3. X-ray crystallography

The suitable crystals of compounds **5**, **5a**, and **6** were crystallized from acetonitrile at room temperature. The crystallographic data are given in Table 1. Crystallographic data were recorded on a Bruker Kappa APEXII CCD area-detector diffractometer using Mo K_α radiation ($\lambda = 0.71073 \text{ \AA}$) at $T = 100(2) \text{ K}$ for **5** and **6** and at $T = 294(2) \text{ K}$ for **5a**. Absorption corrections by multi-scan [39] were applied. Structures were solved by direct methods and refined by full-matrix least squares against F^2 using all data [40]. All non-H atoms were refined anisotropically. H atom positions were calculated geometrically at distances of 0.93 Å (CH), 0.97 Å (CH_2) and 0.96 Å (CH_3) from the parent C atoms; a riding model was used during the refinement

process and the $U_{\text{iso}}(\text{H})$ values were constrained to $1.2U_{\text{eq}}(\text{carrier atom})$ for CH and CH_2 and $1.5U_{\text{eq}}(\text{carrier atom})$ for CH_3 groups.

3. Results and discussion

3.1. Synthesis

The new N/O donor-type bidentate ligands (**3** and **4**) have been prepared by the reduction of the corresponding Schiff bases (**1** and **2**) with NaBH_4 . The reactions of equal amounts of $\text{N}_3\text{P}_3\text{Cl}_6$ with the N/O bifunctional ligands (**3** and **4**) produce N-furan-2-yl-methyl substituted monospirocyclotriphosphazenes (**5** and **6**) in THF. Scheme 1 illustrates the reaction pathway of $\text{N}_3\text{P}_3\text{Cl}_6$ with the ligands for providing a better understanding of the nucleophilic replacement reactions. All the reactions of $\text{N}_3\text{P}_3\text{Cl}_6$ with the bidentate ligands (**3** and **4**) appear to be regioselective because only the spirocyclic arrangements are favored. The reactions of **5** and **6** with excess pyrrolidine, morpholine, and DASD give tetrapyrrolidino (**5a** and **6a**), morpholino (**5b** and **6b**), and 1,4-dioxo-8-azaspiro [4,5] deca (**5c** and **6c**) spirocyclotriphosphazenes, respectively.

Data from the microanalyses, FTIR, APIES-MS and NMR are consistent with the proposed structures of the compounds. While the mass spectra of **5a**, **5b**, **5c**, **6a**, **6b**, and **6c** showed the molecular ion (M^+) peaks, the protonated molecular ion (MH^+) peaks appear in the spectra of **5** and **6**.

3.2. NMR and FTIR spectroscopy

The ^{31}P NMR spectral data of all the compounds refer to the spiro structures. The spin systems of the phosphazenes are interpreted as AX_2 for **5**, **5b**, **5c**, **6**, **6b**, and **6c**, and AB_2 for **5a** and **6a**, give rise to one triplet and one doublet in the ^{31}P NMR spectra. These findings are consistent with the two kinds of P atoms present in the cyclophosphazene ring. The coupling constants, $^2J_{\text{PP}}$, are in the range of 47.5–58.4 Hz. The chemical shift values, $\delta\text{P}(\text{OArN})$, of aminophosphazenes (**5a–6c**) are larger than those of chloro derivatives (**5** and **6**, Table 2), and they are consistent with the findings of N/O donor-type spirocyclotriphosphazenes [41].

In all the spirocyclotriphosphazenes, the ^{13}C and ^1H NMR signals are assigned on the basis of chemical shifts, multiplicities, and coupling constants (Tables 3 and 4). The assignments are made undoubtedly by the HSQC and HMBC (Fig. S1 Supplementary

Table 1
Crystallographic data for **5**, **5a**, and **6**.

	5	5a	6
Empirical formula	$\text{C}_{13}\text{H}_{13}\text{N}_4\text{O}_3\text{P}_3\text{Cl}_4$	$\text{C}_{29}\text{H}_{45}\text{N}_8\text{O}_3\text{P}_3$	$\text{C}_{13}\text{H}_{13}\text{N}_4\text{O}_3\text{P}_3\text{Cl}_4$
Fw	508.01	646.64	507.98
Crystal system	triclinic	triclinic	triclinic
Space group	P-1	P-1	P-1
<i>a</i> (Å)	8.0555(2)	9.9991(8)	7.7561(2)
<i>b</i> (Å)	9.1964(2)	10.9588(9)	8.8500(2)
<i>c</i> (Å)	13.3201(3)	15.4961(12)	14.6474(3)
α (°)	92.392(2)	94.439(3)	97.107(3)
β (°)	98.199(3)	103.033(3)	96.818(3)
γ (°)	93.540(2)	99.123(3)	93.389(2)
<i>V</i> (Å ³)	973.55(4)	1622.0(2)	987.86(4)
<i>Z</i>	2	2	2
μ (cm^{-1})	0.878 (Mo K_α)	0.228 (Mo K_α)	0.866 (Mo K_α)
ρ (calcd) (g cm^{-3})	1.733	1.324	1.708
Number of reflections total	17371	28,194	29,132
Number of reflections unique	4886	8022	4914
R_{int}	0.0431	0.0403	0.0780
$2\theta_{\text{max}}$ (°)	56.90	56.80	56.64
$T_{\text{min}}/T_{\text{max}}$	0.8630/0.9146	0.9265/0.9453	0.7515/0.8811
Number of parameters	245	389	245
$R[F^2 > 2\sigma(F^2)]$	0.0235	0.0570	0.0365
wR	0.0643	0.1338	0.0929

Table 2
 ^{31}P NMR (decoupled) spectral data of the compounds (δ are reported in ppm; J values in Hz).^a

Compound	Spin system	δ (ppm)			$^2J_{\text{PP}}$
		P(OArN)	PCl_2	P(NR) ₂	
5	AX ₂	5.82	23.98	–	58.4
6	AX ₂	5.25	23.87	–	57.5
5a	AB ₂	17.88	–	19.36	47.5
6a	AB ₂	17.57	–	19.09	49.1
5b	AX ₂	16.62	–	22.04	48.5
6b	AX ₂	16.27	–	21.75	49.3
5c	AX ₂	16.16	–	21.71	49.1
6c	AX ₂	15.70	–	21.40	49.5

^a ^{31}P NMR measurements in CDCl_3 solutions at 293 K.

Material). As examples, the HSQC and HMBC spectra of **6a** are illustrated in Fig. S1 (Supplementary Material). The expected carbon signals are assigned from the ^{13}C NMR spectra of all the phosphazenes. The average δ -shift values of C7, C8, NCH_2 (pyrr), NCH_2 (mor), and NCH_2 (DASD) carbons are 48.50, 44.36, 46.10, 44.32, and 42.53 ppm, respectively. Thus, the aromatic and NCH_2 carbon signals of the spirocyclotriphosphazenes are verified by the HSQC and HMBC spectra (Fig. S1 Supplementary Material). The characteristic OCH_3 carbon peaks of all the phosphazenes are observed as singlets at ca. 55.98 ppm. In the ^{13}C NMR spectra of pyrrolidino (**5a** and **6a**), morpholino (**5b** and **6b**), and DASD (**5c** and **6c**) substituted monospirocyclotriphosphazenes, the geminal substituents show two groups of NCH_2CH_2 (pyrr and DASD), OCH_2 (mor and DASD), and OCO (DASD) signals with small separations, indicating

that the two geminal groups are not equivalent to each other (Fig. S2 Supplementary Material). The same situation is also observed for NCH_2 carbons (except **5b**, **6b**, and **6c**). The couplings $^3J_{\text{PC1}}$, $^2J_{\text{PC2}}$ (except **6c**), $^3J_{\text{PC3}}$, and $^3J_{\text{PC9}}$ of the monospirocyclotriphosphazenes are observed as doublets. In addition, the $^2J_{\text{PC2}}$ values of **6a** and **6b** are larger than those of **5a**, **5b**, and **5c**. Additionally, the $^2J_{\text{PC8}}$ values are assigned in the range of 4.0–5.3 Hz, except morpholino derivatives (**5b** and **6b**) (Table 3).

Afterwards, the ^1H NMR spectra of the compounds are evaluated. The benzylic H7 protons give rise to doublets for monospirocyclotriphosphazenes, except **6b** and **6c**, indicating that these protons are equivalent to each other. The geminal H8 protons of all the phosphazenes also give doublets, and the $^3J_{\text{PH}}$ values are between 4.6 and 13.8 Hz. The characteristic OCH_3 peaks of the

Table 3
 ^{13}C NMR (decoupled) spectral data for the phosphazene derivatives. (δ are reported in ppm and J values in Hz).

	Compound							
	5	6	5a	6a	5b	6b	5c	6c
C1	125.00	124.14	125.94	124.52	126.12	124.58	125.81	124.79
C2	$^3J_{\text{PC}} = 7.3$ 149.81	$^3J_{\text{PC}} = 7.1$ 149.73	$^3J_{\text{PC}} = 7.8$ 149.39	$^3J_{\text{PC}} = 7.8$ 152.40	$^3J_{\text{PC}} = 7.7$ 149.29	$^3J_{\text{PC}} = 8.0$ 151.36	$^3J_{\text{PC}} = 7.7$ 149.45	$^3J_{\text{PC}} = 7.8$ 151.63
C3	$^2J_{\text{PC}} = 5.2$ 149.30	$^2J_{\text{PC}} = 5.1$ 119.50	$^2J_{\text{PC}} = 6.3$ 152.51	$^2J_{\text{PC}} = 9.4$ 119.24	$^2J_{\text{PC}} = 6.1$ 151.51	$^2J_{\text{PC}} = 8.4$ 119.06	$^2J_{\text{PC}} = 6.2$ 151.81	$^2J_{\text{PC}} = 6.2$ 119.30
C4	$^3J_{\text{PC}} = 6.9$ 124.34	$^3J_{\text{PC}} = 8.5$ 114.08	$^3J_{\text{PC}} = 8.2$ 122.26	$^3J_{\text{PC}} = 7.7$ 113.32	$^3J_{\text{PC}} = 7.0$ 122.77	$^3J_{\text{PC}} = 7.7$ 113.54	$^3J_{\text{PC}} = 8.2$ 122.28	$^3J_{\text{PC}} = 7.6$ 113.47
C5	112.32	156.01	111.61	154.66	111.21	155.04	111.58	154.82
C6	118.16	111.70	118.90	111.83	118.40	111.95	118.43	111.67
C7	48.20	48.49	48.46	48.82	48.40	48.54	48.40	48.72
C8	$^2J_{\text{PC}} = 1.7$ 44.33	$^2J_{\text{PC}} = 2.0$ 44.38	44.63	44.68	44.64	43.37	44.44	44.43
C9	$^2J_{\text{PC}} = 5.2$ 139.47	$^2J_{\text{PC}} = 5.3$ 143.51	$^2J_{\text{PC}} = 4.4$ 140.67	$^2J_{\text{PC}} = 4.0$ 145.96	140.67	145.12	$^2J_{\text{PC}} = 4.7$ 141.26	$^2J_{\text{PC}} = 4.6$ 145.32
C10	$^3J_{\text{PC}} = 7.9$ 109.18	$^3J_{\text{PC}} = 8.1$ 109.28	$^3J_{\text{PC}} = 8.3$ 108.24	$^3J_{\text{PC}} = 7.5$ 107.92	$^3J_{\text{PC}} = 8.3$ 108.44	$^3J_{\text{PC}} = 7.7$ 108.53	$^3J_{\text{PC}} = 8.1$ 108.37	$^3J_{\text{PC}} = 8.0$ 108.44
C11	110.44	110.48	110.15	110.20	110.23	110.24	110.11	110.13
C12	142.91	142.96	142.37	141.86	142.31	142.37	142.22	142.26
OCH_3	56.46	55.71	56.52	55.72	55.89	55.62	56.27	55.63
OCH_2	–	–	–	–	67.19	67.15	64.15	64.20
$\text{N-CH}_2\text{-CH}_2$	–	–	25.58	26.32	–	–	35.52	35.55
			$^3J_{\text{PC}} = 8.4$ 26.62	$^3J_{\text{PC}} = 8.0$ 26.38			$^3J_{\text{PC}} = 6.7$ 35.60	$^3J_{\text{PC}} = 6.4$ 35.56
NCH_2	–	–	$^3J_{\text{PC}} = 8.3$ 46.04	$^3J_{\text{PC}} = 8.1$ 46.04	44.64	44.00	$^3J_{\text{PC}} = 6.9$ 42.54	$^3J_{\text{PC}} = 6.5$ 42.42
OCO	–	–	46.13	46.18	–	–	42.63	42.63
			–	–	–	–	107.62	107.59
							107.86	107.77

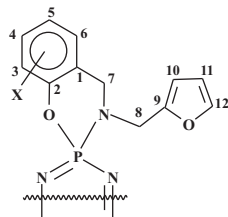


Table 4¹H NMR spectral data for **2–6**, **5a–5c**, and **6a–6c** [s: singlet, d: doublet, dd: doublet of doublets, m: multiplet, and bp: broad peak].^a

	Compound[δ (ppm), J(Hz)]										
	2	3	4	5	6	5a	6a	5b	6b	5c	6c
H3	6.92 (d, 1H) ³ J _{H3-H4} = 9.0	–	6.81 (d, 1H) ³ J _{H3-H4} = 8.8	–	6.99 (d, 1H) ³ J _{H3-H4} = 8.9	–	6.81 (d, 1H) ³ J _{H3-H4} = 7.9	–	6.82 (d, 1H) ³ J _{H3-H4} = 8.8	–	6.89 (d, 1H) ³ J _{H3-H4} = 8.8
H4	6.95 (dd, 1H) ³ J _{H3-H4} = 9.0 ⁴ J _{H4-H6} = 2.6	6.85 (dd, 1H) ³ J _{H4-H5} = 8.1 ⁴ J _{H4-H6} = 1.4	6.76 (dd, 1H) ³ J _{H3-H4} = 8.8 ⁴ J _{H4-H6} = 2.9	6.88 (d, 1H) ³ J _{H4-H5} = 8.2	6.77 (dd, 1H) ³ J _{H3-H4} = 8.9 ⁴ J _{H4-H6} = 2.5	6.75(d, 1H) ³ J _{H4-H5} = 8.0	6.67(d, 1H) ³ J _{H3-H4} = 7.9 ⁴ J _{H4-H6} = 2.9	6.81(d, 1H) ³ J _{H4-H5} = 8.1	6.70 (dd, 1H) ³ J _{H3-H4} = 8.8 ⁴ J _{H4-H6} = 2.5	6.77 (d, 1H) ³ J _{H4-H5} = 8.5	6.70 (dd, 1H) ³ J _{H3-H4} = 8.8 ⁴ J _{H4-H6} = 2.8
H5	–	6.78 (dd, 1H) ³ J _{H4-H5} = 8.1 ³ J _{H5-H6} = 7.6	–	7.01 (dd, 1H) ³ J _{H4-H5} = 8.2 ³ J _{H5-H6} = 7.8	–	6.85(dd, 1H) ³ J _{H4-H5} = 8.0 ³ J _{H5-H6} = 7.7	–	6.93 (dd, 1H) ³ J _{H4-H5} = 8.1 ³ J _{H5-H6} = 7.7	–	6.88 (dd, 1H) ³ J _{H4-H5} = 8.5 ³ J _{H5-H6} = 7.8	–
H6	6.80 (d, 1H) ⁴ J _{H4-H6} = 2.6	6.68 (dd, 1H) ³ J _{H5-H6} = 7.6 ⁴ J _{H4-H6} = 1.4	6.58 (d, 1H) ⁴ J _{H4-H6} = 2.9	6.65 (d, 1H) ³ J _{H5-H6} = 7.8	6.57 (d, 1H) ⁴ J _{H4-H6} = 2.5	6.56 (d, 1H) ³ J _{H5-H6} = 7.7	6.51(d, 1H) ⁴ J _{H4-H6} = 2.9	6.60 (d, 1H) ³ J _{H5-H6} = 7.7	6.54 (d, 1H) ⁴ J _{H4-H6} = 2.5	6.59 (d, 1H) ³ J _{H5-H6} = 7.8	6.53 (d, 1H) ⁴ J _{H4-H6} = 2.8
H7	8.35 (s, 1H)	3.87 (s, 2H)	3.83 (s, 2H)	4.27 (d, 2H) ³ J _{PH} = 11.8	4.26 (d, 2H) ³ J _{PH} = 3.5	4.20 (d, 2H) ³ J _{PH} = 13.8	4.18 (d, 2H) ³ J _{PH} = 14.6	4.24 (d, 2H) ³ J _{PH} = 2.4	4.20 (s, 2H)	4.18 (d, 2H) ^{2H} ³ J _{PH} = 2.5	4.17 (s, 2H)
H8	4.78 (s, 2H)	4.00 (s, 2H)	3.94 (s, 2H)	4.29 (d, 2H) ³ J _{PH} = 13.8	4.29 (d, 2H) ³ J _{PH} = 5.7	4.24 (d, 2H) ³ J _{PH} = 8.4	4.26 (d, 2H) ³ J _{PH} = 7.3	4.21 (d, 2H) ³ J _{PH} = 7.5	4.27 (d, 2H) ³ J _{PH} = 5.2	4.21 (d, 2H) ³ J _{PH} = 8.3	4.20 (d, 2H) ³ J _{PH} = 4.6
H10	6.30 (m, 1H) ³ J _{H10-H11} = 3.3 ⁴ J _{H10-H12} = 1.9	6.27 (m, 1H) ³ J _{H10-H11} = 3.1 ⁴ J _{H10-H12} = 1.8	6.23 (d, 1H) ³ J _{H10-H11} = 3.1	6.35 (m, 1H) ³ J _{H10-H11} = 3.2 ⁴ J _{H10-H12} = 1.8	6.37 (m, 1H)	6.31 (m, 1H)	6.28 (m, 1H)	6.31 (m, 1H) ³ J _{H10-H11} = 3.1	6.28 (m, 1H) ³ J _{H10-H11} = 3.1 ⁴ J _{H10-H12} = 1.7	6.31 (m, 1H)	6.32 (m, 1H) ³ J _{H10-H11} = 3.2 ³ J _{H10-H12} = 1.5
H11	6.38 (m, 1H) ³ J _{H10-H11} = 3.3 ³ J _{H11-H12} = 3.2	6.36 (m, 1H) ³ J _{H10-H11} = 3.1 ³ J _{H11-H12} = 2.5	6.36 (m, 1H) ³ J _{H10-H11} = 3.1 ³ J _{H11-H12} = 2.0	6.35 (m, 1H) ³ J _{H10-H11} = 3.2 ³ J _{H11-H12} = 2.7	6.37 (m, 1H)	6.31 (m, 1H) ³ J _{H11-H12} = 1.2	6.30 (m, 1H)	6.34 (m, 1H) ³ J _{H10-H11} = 3.1 ³ J _{H11-H12} = 1.9	6.32 (m, 1H) ³ J _{H10-H11} = 3.1 ³ J _{H11-H12} = 2.8	6.31 (m, 1H)	6.33 (m, 1H) ³ J _{H10-H11} = 3.2 ³ J _{H11-H12} = 2.8
H12	7.40 (m, 1H) ³ J _{H11-H12} = 3.2 ⁴ J _{H10-H12} = 1.9	7.40 (m, 1H) ³ J _{H11-H12} = 2.5 ⁴ J _{H10-H12} = 1.8	7.41 (m, 1H) ³ J _{H11-H12} = 2.0	7.40 (m, 1H) ³ J _{H11-H12} = 2.7 ⁴ J _{H10-H12} = 1.8	7.41 (m, 1H)	7.35 (m, 1H) ³ J _{H11-H12} = 1.2	7.35 (m, 1H)	7.38 (m, 1H) ³ J _{H11-H12} = 1.9	7.35 (m, 1H) ³ J _{H11-H12} = 2.8 ⁴ J _{H10-H12} = 1.7	7.39 (m, 1H)	7.39 (m, 1H) ³ J _{H11-H12} = 2.8 ³ J _{H10-H12} = 1.5
OCH ₃	3.79 (s, 3H)	3.90 (s, 3H)	3.76 (s, 3H)	3.88 (s, 3H)	3.76 (s, 3H)	3.79 (s, 3H)	3.73 (s, 3H)	3.82 (s, 3H)	3.72 (s, 3H)	3.82 (s, 3H)	3.74 (s, 3H)
OCH ₂	–	–	–	–	–	–	–	3.65 (t, 8H) ³ J _{HH} = 8.9 3.69 (t, 8H) ³ J _{HH} = 8.4	3.62 (t, 8H) ³ J _{HH} = 8.5 3.65 (t, 8H) ³ J _{HH} = 9.1	3.96 (s, 8H) 3.97 (s, 8H)	3.96 (s, 8H) 3.97 (s, 8H)
N–CH ₂ –CH ₂	–	–	–	–	–	1.77 (t, 8H) ³ J _{HH} = 6.9 1.80 (t, 8H) ³ J _{HH} = 6.1	1.76 (t, 8H) ³ J _{HH} = 6.7 1.82 (t, 8H) ³ J _{HH} = 7.6	–	–	1.63–1.70 (m, 16H)	1.65 (t, 8H) ³ J _{HH} = 5.6 1.69 (t, 8H) ³ J _{HH} = 5.6
NCH ₂	–	–	–	–	–	3.13 (m,8H) 3.19 (m,8H)	3.10 (m,8H) 3.18 (m,8H)	3.12–3.26 (m, 16H)	3.07–3.19 (m, 16H)	3.06–3.40 (m, 16H)	3.23–3.28 (m, 16H)
OH	12.85 (bp, 1H)	–	–	–	–	–	–	–	–	–	–

^a Numberings of protons are given in Table 3.

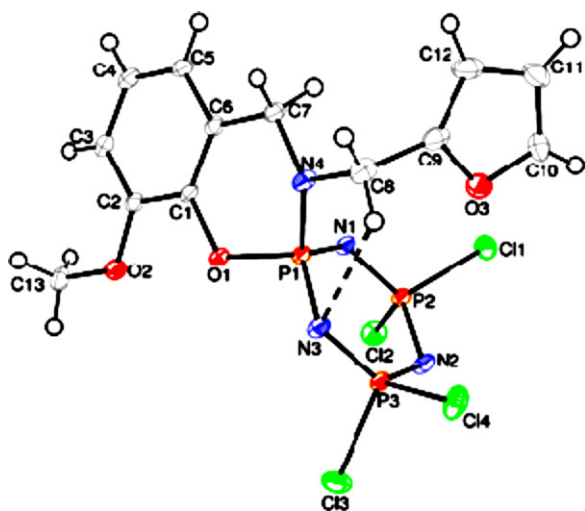


Fig. 1. ORTEP-3 [48] drawing of **5** with the atom-numbering scheme. Displacement ellipsoids are drawn at the 50% probability level.

ligands (**2**, **3** and **4**) and all the phosphazenes are observed as singlets at ca. 3.79 ppm. In the ^1H NMR spectra of pyrrolidino (**5a** and **6a**), morpholino (**5b** and **6b**), and DASD (**5c** and **6c**) substituted monospirocyclotriphosphazenes, the geminal substituents show two groups of NCH_2 signals with small separations, as it is observed in the ^{13}C NMR spectra. The same situation is also observed for NCH_2CH_2 (pyrr and DASD) and OCH_2 (mor and DASD) protons (Fig. S2 Supplementary Material). The average values of $^3J_{\text{HH}}$ and $^4J_{\text{HH}}$ for benzene rings are 8.2 Hz and 2.5 Hz, respectively. In addition, the $^3J_{\text{HH}}$ values of furan rings of all the compounds are very smaller than those of benzene rings (Table 4).

The FTIR spectra of the ligands (**3** and **4**) and all the phosphazenes show two medium intensity absorption bands at $3117\text{--}3071\text{ cm}^{-1}$ and $3076\text{--}3046\text{ cm}^{-1}$ attributed to asymmetric and symmetric stretching vibrations of the Ar-H protons. In addition, all the phosphazenes exhibit intense bands between 1255 and 1156 cm^{-1} related to $\nu_{\text{P-N}}$ bonds of the phosphazene rings [42]. The characteristic ν_{NH} stretching bands of N-alkyl(or aryl)-o-hydroxybenzylamines (3301 cm^{-1} for **3** and 3289 cm^{-1} for **4**) disappear in the FTIR spectra of monospirocyclotriphosphazenes. As expected, $\nu_{\text{PCl}_2(\text{asym})}$ and $\nu_{\text{PCl}_2(\text{sym})}$ bands emerge at 564 and 527 cm^{-1} for **5**, and 581 and 519 cm^{-1} for **6**.

3.3. X-ray structures of **5**, **5a**, and **6**.

The molecular and solid-state structures of **5**, **5a**, and **6** along with the atom-numbering schemes, are depicted in Figs. 1–3, respectively. The selected bond lengths and angles are listed in Table 5 and hydrogen-bond data are given in Table 6. The phosphazene rings of **5** and **6** are nearly planar (Fig. S3a Supplementary Material); $\varphi_2 = -22.6(0.8)^\circ$, $\theta_2 = 99.6(0.8)^\circ$, Fig. S5a (Supplementary Material); $\varphi_2 = -147.8(5.7)^\circ$, $\theta_2 = 15.7(1.5)^\circ$, while that of **5a** is not planar, and it is in twisted-boat conformation (Fig. S4a Supplementary Material); $\varphi_2 = -153.0(0.6)^\circ$, $\theta_2 = 123.2(0.5)^\circ$ having total puckering amplitudes Q_{T} of $0.067(1)\text{ \AA}$ (for **5**), $0.178(2)\text{ \AA}$ (for **5a**) and $0.050(1)\text{ \AA}$ (for **6**) [43]. In tetrachloro monospirocyclotriphosphazene (**5**), the six-membered ring P1/O1/C1/C6/C7/N4 is in boat conformation (Fig. S3b Supplementary Material); $Q_{\text{T}} = 1.221(3)\text{ \AA}$, $\varphi_2 = 128.3(1)^\circ$, $\theta_2 = 77.0(1)^\circ$, and in **5a** and **6**, the six-membered rings, P1/O1/C1/C6/C7/N4, are in twisted conformations (Fig. S4b Supplementary Material); $Q_{\text{T}} = 0.705(2)\text{ \AA}$, $\varphi_2 = 44.9(3)^\circ$, $\theta_2 = 35.5(2)^\circ$ and Fig. S5b (Supplementary Material); $Q_{\text{T}} = 1.471(4)\text{ \AA}$, $\varphi_2 = -66.7(1)^\circ$, $\theta_2 = 122.1(1)^\circ$.

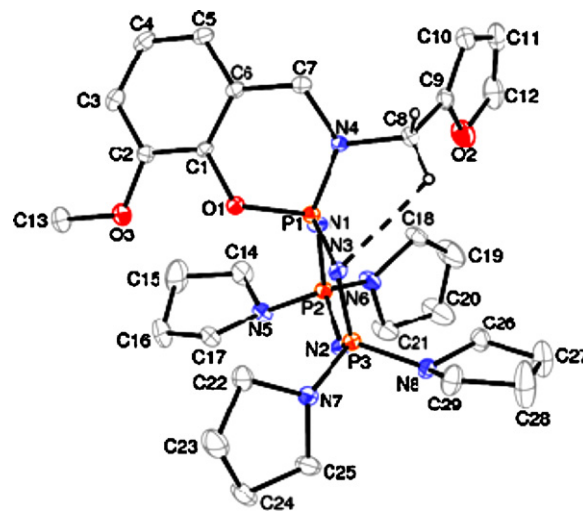


Fig. 2. ORTEP-3 [48] drawing of **5a** with the atom-numbering scheme. Displacement ellipsoids are drawn at the 50% probability level.

Table 5
Selected bond lengths (Å) and angles ($^\circ$) for **5**, **5a**, and **6**.

	5	5a	6
P1–N1	1.605(1)	1.583(2)	1.604(2)
P1–N3	1.592(1)	1.577(2)	1.594(2)
P1–N4	1.613(3)	1.641(2)	1.631(2)
P1–O1	1.587(1)	1.621(2)	1.583(2)
P2–N1	1.565(1)	1.600(2)	1.557(2)
P2–N2	1.589(1)	1.589(2)	1.587(2)
P3–N2	1.579(1)	1.590(2)	1.584(2)
P3–N3	1.574(1)	1.606(2)	1.567(2)
N1–P1–N3	116.2(1)	116.7(1)	114.8(1)
N1–P2–N2	118.8(1)	115.8(1)	119.4(1)
N2–P3–N3	120.5(1)	116.4(1)	120.3(1)
N4–P1–O1	101.7(1)	100.5(1)	102.7(1)
P1–N1–P2	123.1(1)	122.1(1)	123.7(1)
P2–N2–P3	119.5(1)	123.6(1)	118.8(1)
P1–N3–P3	121.5(2)	122.2(1)	122.7(1)
N5–P2–N6	–	100.6(1)	–
N7–P3–N8	–	101.4(2)	–

In the phosphazene rings of **5**, **5a**, and **6**, the endocyclic P–N bond lengths are in the ranges of $1.565(1)\text{--}1.605(1)\text{ \AA}$ (for **5**), $1.577(2)\text{--}1.606(2)\text{ \AA}$ (for **5a**), and $1.557(2)\text{--}1.604(2)\text{ \AA}$ (for **6**) and there are regular variations with the distances from P1: P1–N1 \approx P1–N3 > P2–N2 \approx P3–N2 > P2–N1 \approx P3–N3. In addition,

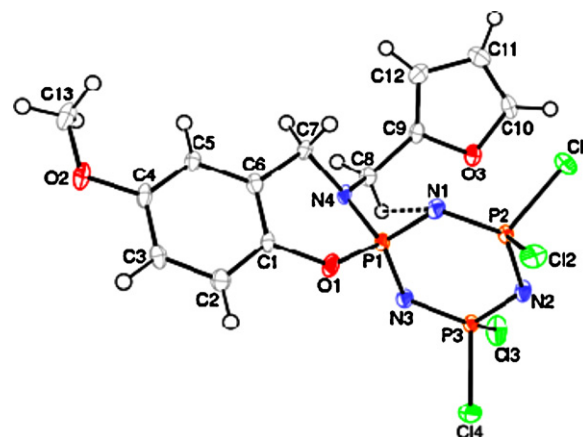


Fig. 3. ORTEP-3 [48] drawing of **6** with the atom-numbering scheme. Displacement ellipsoids are drawn at the 50% probability level.

Table 6
Hydrogen-bond geometries (Å,°) for **5**, **5a**, and **6**.

D-H...A	D-H	H...A	D...A	D-H...A	
5	C8–H8A...N3	0.97	2.61	3.092(4)	111
5a	C8–H8A...N3	0.97	2.63	3.114(4)	110
	C12–H12...O3 ⁱ	0.93	2.51	3.291(4)	142
6	C8–H8B...N3	0.97	2.72	3.144(3)	107

Symmetry code: (i) $x+1, y, z$.

the average endocyclic P–N bond lengths in phosphazene rings are 1.584(1) and 1.591(2), and 1.582(2) Å, which are shorter than the exocyclic P–N bonds of **5**, **5a**, and **6**, respectively (Table 5). It is noteworthy that, the P–N bonds are thought to be the most intriguing bonds in chemistry. In recent years, natural bond orbital (NBO) and topological electron density analyses have been used to investigate the electronic structures of the phosphazenes [44]. The two kinds of phosphazene bonding alternatives are suggested, namely negative hyperconjugation [44,45] and ionic bonding, which are scrutinized using NBO. The estimations imply that the ionic component is the dominant feature. However, these two alternatives are not mutually exclusive and in fact, they are both important. The major donor-acceptor interactions (NBO overlaps) are depicted in Fig. 4 for $N_3P_3Cl_6$, taken from reference 44. In addition, the presence of the negative hyperconjugation strongly contribute to the multiple-bond character, and the electron withdrawing or releasing substituents bonding to the P atoms increase or decrease the negative hyperconjugation of the exocyclic and endocyclic P–N bonds. Consequently, the shortenings of the endo- and exocyclic P–N bonds in **5**, **5a**, and **6** could be explained by the negative hyperconjugation concept.

In monospirocyclic phosphazenes (**5**, **5a**, and **6**), the endocyclic N1–P1–N3 (α) angles are considerably narrowed, while the exocyclic O1–P1–N4 (α') angles are hardly changed with respect to the corresponding values in the “standard” compound, $N_3P_3Cl_6$ (Table 5). In $N_3P_3Cl_6$, the α and α' angles are 118.3(2) and 101.2(1)°, respectively [46]. It is suggested that the negative hyperconjugation and substituent-dependent charge at the P centers play an important role in the variations of exocyclic and endocyclic angles. The charge separations between the P and N atoms in the phosphazene rings differ significantly depending on the electron withdrawing or releasing capacities of the substituents bonded to the P atoms [47]. The narrowing of the endocyclic NPN (α) angles in **5**, **5a**, and **6** could also be explained by the negative hyperconjugation concept.

On the other hand, compounds **5**, **5a**, and **6** have intramolecular C–H...N hydrogen bonds (Table 6) between furanyl-CH₂ and nitrogen atoms of phosphazene rings (Figs. 1–3), indicating that the CH₂ protons of these compounds have acidic properties. In compound **5a**, intermolecular C–H...O hydrogen bonds link the molecules into a two-dimensional network. The π ... π contacts between the benzene rings, Cg1...Cg1ⁱ [for **5**, (i) 2–x, –y, –z], Cg1...Cg1ⁱⁱ [for **5a**, (ii) 1–x, 2–y, 1–z] and Cg1...Cg1ⁱⁱⁱ [for **6**, (iii) 2–x, 1–y, 1–z] [where Cg1 is the centroid of the ring (C1–C6)] with the centroid–centroid distances of 3.532(1) Å (for **5**), 3.939(2) Å (for **5a**), and 3.899(1) Å (for **6**). In compound **5a**, there is also a π ... π contact between the furan rings, Cg2...Cg2^{iv} [(iv) –x, 1–y, 1–z, where Cg2 is the centroid of the ring (O2/C9–C12)] with centroid–centroid distance of 3.534(2) Å.

3.4. Antibacterial activity

The pyrrolidine and the morpholine derivatives, and some of the organic compounds containing furan side groups have widespread structural features of natural and synthetic biologically designed active molecules, and they can be used for pharmaceutical and medicinal purposes [43–51]. The herbicidal, plant growth regulatory, fungicidal, anti-microbial, anti-inflammatory, and anti-cancer activities of these heterocycles have been known in the literature [52–55]. So, furan, pyrrolidine, and morpholine are especially chosen as the substituents in this study.

The antibacterial activity of **5a**, **5b**, **5c**, **6a**, **6b**, and **6c** are determined against eight different microorganisms [*Staphylococcus aureus* ATCC 25923 (G+), *Pseudomonas aeruginosa* ATCC 27853 (G–), *Escherichia coli* ATCC 25922 (G–), *Bacillus subtilis* ATCC 6633 (G+), *Bacillus cereus* NRRL-B-3711 (G+), and *Enterococcus faecalis* ATCC 292112 (G+), *Candida albicans* ATCC 10231 and *Candida tropicalis* ATCC 13803]. All the compounds with 5000 μ M and 10,000 μ M concentrations exhibit no antimicrobial activity. Moreover,

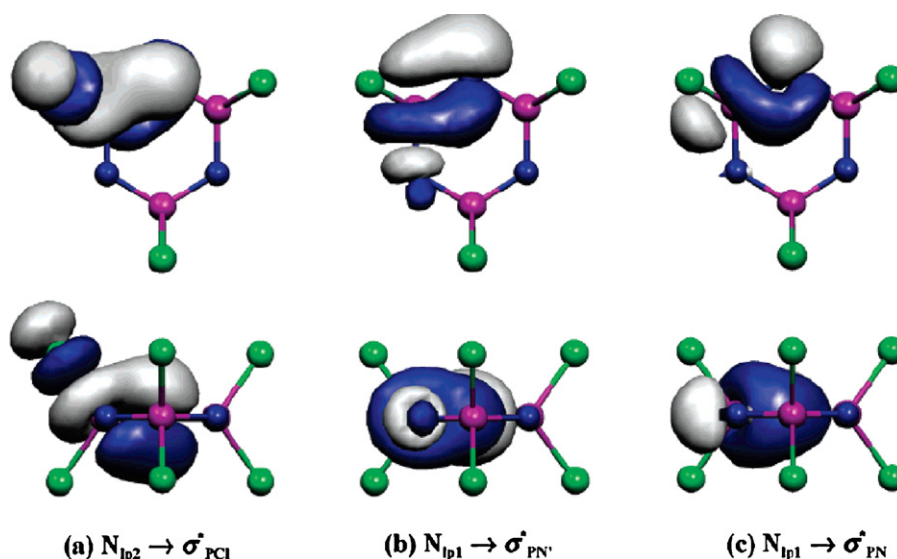


Fig. 4. Major NBO overlaps in $N_3P_3Cl_6$: (a) $N_{lp2} \rightarrow \sigma^*_{PCl}$, (b) $N_{lp1} \rightarrow \sigma^*_{PN'}$, and (c) $N_{lp1} \rightarrow \sigma^*_{PN}$.

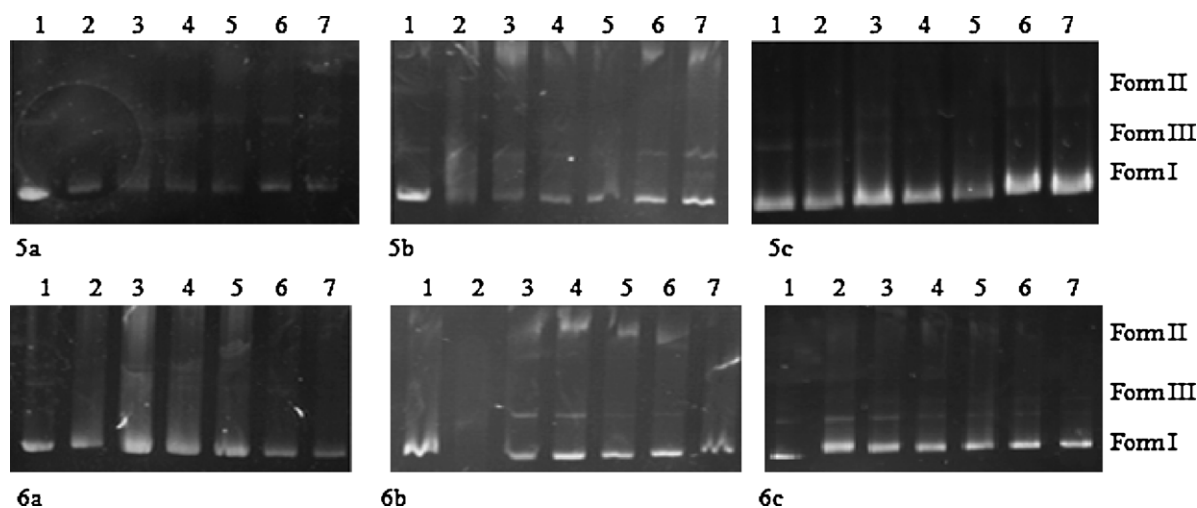


Fig. 5. Agarose gel electrophoresis of pBR322 plasmid DNA with the compounds **5a**, **5b**, **5c**, **6a**, **6b**, and **6c** of different concentrations. Lane 1: untreated plasmid DNA as a control, lanes 2–6: plasmid DNA treated with different concentrations of compound ranging from (5000, 2500, 1250, 625, and 125 μM).

pyrrolidine, morpholine, DASD, and 2-furan-2-yl-methylamine, which are the substituents of the N/O spirocyclotriphosphazenes, are tested against the same bacteria and fungi. However, no activities have been observed against the tested bacteria and fungi. The reason for that could be protective outer membrane of microorganisms. All of the antimicrobial agents demonstrate selective toxicity towards the bacteria and fungi. Antibiotics or any antimicrobial agent may inhibit protein, DNA, and folic acid syntheses. The resistance to antibiotics or the compounds may attribute to the inability of the molecules to enter into the cell or after entering export from the cell. In addition, the resistance of microorganisms may be depend on the production of an enzyme by the cell to inactivate the compounds.

3.5. Interactions of DNA with the compounds

Agarose gel electrophoresis is used to demonstrate the conformational change and damage caused to plasmid DNA, due to their bindings with the compounds. When the plasmid DNA loads on the gel in an electric field, the plasmid DNA will migrate towards the positive electrode. The plasmid DNA is found in three different forms, supercoiled circular form I, singly nicked relaxed circular form II, and doubly nicked linear form III. Generally, the untreated plasmid DNA migrates on the gel with two DNA bands, which form I migrating faster and form II migrating slower. Form III takes place in the middle when plasmid DNA restricted with the enzyme or damage. Interactions with compounds may cause conformational changes on the plasmid DNA, and in mobility of DNA through gel [56,57]. Therefore, gel electrophoresis has been carried out using agarose gel in order to investigate the abilities of **5a**, **5b**, **5c**, **6a**, **6b**, and **6c** in effecting the plasmid DNA pBR322 DNA. Fig. 5 shows the gel electrophoresis of plasmid pBR322 DNA after 24 h incubation in the presence of the compounds. The concentrations of the compounds are 5000, 2500, 1250, 625, and 125 μM. It is observed that all the compounds exhibit the effect in more or less, dose dependent manner. In addition, compounds **5c** and **6c** exhibit different effects of all the concentrations on plasmid DNA than the other tested compounds. In the case of **5a**, the mobilities of the bands of supercoiled DNA decrease slightly at concentration of 5000 μM. The intensities of these bands also decrease. In all the concentrations, compound **6a** has considerable effects on supercoiled plasmid DNA, but the maximum effect is observed at the concentration of 5000 μM. It is noteworthy that the effect of **5b** is highly noticeable in three high concentrations. The intensity of the

supercoiled plasmid DNA decreases with the increasing concentrations of **5b**. Moreover, the effect of **6b** is maximum at the highest concentration of the compound. When the DNA cleavage assay for the compound **5c** is examined, the mobility of Form I decreases with the decreasing concentrations of the compound. The intensity of Form II diminishes with the decreasing concentrations of **5c** (lanes 2–6). It can be seen that Form I of supercoiled plasmid DNA diminishes gradually with decreasing concentrations of **5c**, whereas the intensity of Form III increases. It appears that the compound cleaves the supercoiled Form I DNA to linear Form III. In the case of **6c**, the mobility of the supercoiled DNA slightly decreases with the increasing concentrations of the compound. It is clearly understood that compound **6c** also causes the conformational changes on pBR322 plasmid DNA by cleaving supercoiled DNA to linear Form III, as compound **5c**.

Consequently, the activities of the compounds are considered to be associated with their bindings with nucleotides in DNA, in which they cause some changes in DNA conformations or damage to DNA. Binding modes are possible intercalatives as all of the compounds are aromatic and also have hydrogen bond donors/acceptors [58]. DNA is a very valuable target for the actions of many anticancer agents. Therefore, it is very important to find out whether the compound can bind to DNA, and the binding may suppress its function. So, DNA targeted compounds offer opportunity for development of new anticancer agents. The results obtained in this study could provide the important scientific knowledge for scientists interesting in this field.

4. Conclusions

The spirocyclotriphosphazene derivatives containing 1,3,2-oxazaphosphorine rings are very limited in the literature. In this study, new tetrachloro (**5** and **6**), tetrapyrrolidino (**5a** and **6a**), tetramorpholino (**5b** and **6b**), and tetra(1,4-dioxo-8-azaspiro[4,5]deca) (**5c** and **6c**) monospirocyclotriphosphazenes have been obtained. The molecular and solid-state structures of **5**, **5a**, and **6** are determined by X-ray crystallography, and the phosphazene rings of **5** and **6** are nearly in planar and the other one is in twisted-boat conformations. In addition, the compounds **5a**, **5b**, **5c**, **6a**, **6b**, and **6c** have no antimicrobial activities. Interactions between these compounds and pBR322 plasmid DNA show that the compounds are effective in changing the mobility of the DNA.

Acknowledgements

The authors thank the “Medicinal Plants and Medicine Research Center of Anadolu University, Eskişehir” for the use of their X-ray and NMR facilities. L.A. grateful to State Planning Organisation for financial support for the research Project number 1998K121480. T.H. is indebted to “Hacettepe University, Scientific Research Unit” (Grant 02 02 602 002) for their financial support.

Appendix A. Supplementary data

Supplementary data associated with this article can be found, in the online version, at doi:10.1016/j.saa.2011.10.027.

References

- [1] V. Chandrasekhar, P. Thilagar, B.M. Pandian, *Coord. Chem. Rev.* 251 (2007) 1045–1074.
- [2] H. Dal, S. Safran, Y. Süzen, T. Hökelek, Z. Kılıç, *J. Mol. Struct.* 753 (2005) 89–96.
- [3] H.R. Allcock, *Chemistry and Applications of Polyphosphazenes*, John Wiley and Sons, 2003.
- [4] S. Beşli, M. Durmuş, H. İbişoğlu, A. Kılıç, F. Yüksel, *Polyhedron* 29 (2010) 2609–2618.
- [5] S.R. Contractor, Z. Kılıç, R.A. Shaw, *J. Chem. Soc. Dalton Trans.* (1987) 2023–2029.
- [6] S.W. Bartlett, S.J. Coles, D.B. Davies, M.B. Hursthouse, H. İbişoğlu, A. Kılıç, R.A. Shaw, *Acta Crystallogr. B62* (2006) 321–329.
- [7] N. Asmafiliz, E.E. İlter, M. Işıklan, Z. Kılıç, B. Tercan, N. Çaylak, T. Hökelek, O. Büyükgüngör, *J. Mol. Struct.* 30 (2007) 172–183.
- [8] E.E. İlter, N. Asmafiliz, Z. Kılıç, M. Işıklan, T. Hökelek, N. Çaylak, E. Şahin, *Inorg. Chem.* 46 (2007) 9931–9944.
- [9] N. Asmafiliz, Z. Kılıç, A. Öztürk, T. Hökelek, L.Y. Koç, L. Açık, Ö. Kısa, A. Albay, Z. Üstündağ, A.O. Solak, *Inorg. Chem.* 48 (2009) 10102–10116.
- [10] S. Bilge, Ş. Demiriz, A. Okumuş, Z. Kılıç, B. Tercan, T. Hökelek, O. Büyükgüngör, *Inorg. Chem.* 45 (2006) 8755–8767.
- [11] N.N. Bhuvan Kumar, K.C. Kumara Swamy, *Chirality* 20 (2008) 781–789.
- [12] N. Satish Kumar, K.C. Kumara Swamy, *Polyhedron* 23 (2004) 979–985.
- [13] M. Yıldız, D. Erdener, H. Ünver, N. Ocak İskeleli, *J. Mol. Struct.* 753 (2005) 165–172.
- [14] S. Kumaraswamy, M. Vijjulatha, C. Muthiah, K.C. Kumara Swamy, U. Engelhardt, *J. Chem. Soc. Dalton Trans.* (1999) 891–900.
- [15] P. Kommana, S. Kumaraswamy, K.C. Kumara Swamy, *Inorg. Chem. Commun.* 6 (2003) 394–397.
- [16] S. Beşli, H. İbişoğlu, A. Kılıç, İ. Ün, F. Yüksel, *Polyhedron* 29 (2010) 3220–3228.
- [17] I. Dez, J. Levalois-Mitjaville, H. Grützmacher, V. Gramlinch, R. Jaeger, *Eur. J. Inorg. Chem.* (1999) 1673–1684.
- [18] D. Mathew, C.P. Nair, K.N. Ninan, *Polym. Int.* 49 (2000) 48–56.
- [19] H.R. Allcock, U. Diefenbach, S.R. Pucher, *Inorg. Chem.* 33 (1994) 3091–3095.
- [20] M. Işıklan, Ö. Sonkaya, B. Çoşut, S. Yeşilot, T. Hökelek, *Polyhedron* 29 (2010) 1612–1618.
- [21] M. Siwy, D. Şek, B. Kaczmarczyk, I. Jaroszewicz, A. Nasulewicz, M. Pelczyńska, D. Nevozhay, A. Opolski, *J. Med. Chem.* 49 (2006) 806–810.
- [22] E.E. İlter, N. Asmafiliz, Z. Kılıç, L. Açık, M. Yavuz, E.B. Bali, A.O. Solak, F. Büyükkaya, H. Dal, T. Hökelek, *Polyhedron* 29 (2010) 2933–2944.
- [23] K. Brandt, T.J. Bartczak, R. Kruszynski, I. Porwollik-Czomperlik, *Inorg. Chim. Acta* 322 (2001) 138–144.
- [24] X. Zhu, Y. Liang, D. Zhang, L. Wang, Y. Ye, Y. Zhao, *Phosphorus Sulfur Silicon Relat. Elem.* 186 (2011) 281–286.
- [25] B.A. Omotowa, B.S. Phillips, J.S. Zabinski, J.M. Shreeve, *Inorg. Chem.* 43 (2004) 5466–5471.
- [26] J. Barbera, M. Bardaji, J. Jimenez, A. Laguna, M.P. Martinez, L. Oriol, J.L. Serrano, I. Zaragoza, *J. Am. Chem. Soc.* 127 (2005) 8994–9002.
- [27] R. Schneider, C. Köllner, I. Weber, A. Togni, *Chem. Commun.* 23 (1999) 2415–2416.
- [28] R. Lui, X. Wang, *Polym. Degrad. Stab.* 94 (2009) 617–624.
- [29] J.F. Kuan, K.F. Lin, *J. Appl. Polym. Sci.* 91 (2004) 697–702.
- [30] J. Ding, H. Liang, W. Shi, X. Shen, *J. Appl. Polym. Sci.* 97 (2005) 1776–1782.
- [31] H.R. Allcock, M.E. Napierala, C.G. Cameron, S.J.M. O’Connor, *Macromolecules* 29 (1996) 1951–1956.
- [32] H.R. Allcock, *Curr. Opin. Solid State Mater. Sci.* 10 (2006) 231–240.
- [33] G. Xu, Q. Lu, B. Yu, L. Wen, *Solid State Ionics* 177 (2006) 305–309.
- [34] D.A. Conner, D.T. Welna, Y. Chang, H.R. Allcock, *Macromolecules* 40 (2007) 322–328.
- [35] Y.E. Greish, J.D. Bender, S. Lakshmi, P.W. Brown, H.R. Allcock, C.T. Laurencin, *Biomaterials* 26 (2005) 1–9.
- [36] L. Nair, S. Bhattacharyya, J.D. Bender, Y.E. Greish, P.W. Brown, H.R. Allcock, C.T. Laurencin, *Biomacromolecules* 5 (2004) 2212–2220.
- [37] Bruker program 1D WIN-NMR (release 6.0) and 2D WIN-NMR (release 6.1).
- [38] H. Ünver, Z. Hayvalı, *Spectrochim. Acta A75* (2010) 782–788.
- [39] Bruker, SADABS, Bruker AXS Inc., Madison, WI, USA, 2005.
- [40] G.M. Sheldrick, SHELXS-97; SHELXL-97, University of Göttingen, Göttingen, Germany, 1997.
- [41] M. Işıklan, N. Asmafiliz, E.E. Özalp, E.E. İlter, Z. Kılıç, B. Çoşut, S. Yeşilot, A. Kılıç, A. Öztürk, T. Hökelek, L.Y. Koç Bilir, L. Açık, E. Akyüz, *Inorg. Chem.* 49 (2010) 7057–7071.
- [42] G.A. Carriedo, F.G. Alonso, P.A. Gonzalez, J.R. Menendez, *J. Raman Spectrosc.* 29 (1998) 327–330.
- [43] D. Cremer, J.A. Pople, *J. Am. Chem. Soc.* 97 (1975) 1354–1358.
- [44] A.B. Chaplin, J.A. Harrison, P.J. Dyson, *Inorg. Chem.* 44 (2005) 8407–8417.
- [45] S.S. Krishnamurthy, *Phosphorus Sulfur Silicon Relat. Elem.* 87 (1994) 101–111.
- [46] G.J. Bullen, *J. Chem. Soc. A* (1971) 1450–1453.
- [47] V. Luaña, A.M. Pendás, A. Costales, G.A. Carriedo, F.J. García-Alonso, *J. Phys. Chem. A* 105 (2001) 5280–5291.
- [48] L.J. Farrugia, *J. Appl. Crystallogr.* 30 (1997) 565–566.
- [49] Y. Liu, B. Cai, Y. Li, H. Song, R. Huang, Q. Wang, *J. Agric. Food Chem.* 55 (2007) 3011–3017.
- [50] F. Bellina, R. Rossi, *Tetrahedron* 62 (2006) 7213–7256.
- [51] E.G. Mesropyan, G.B. Ambartsumyan, A.A. Avetisyan, A.S. Galstyan, A.N. Kirakosyan, *Chem. Heterocycl. Compd.* 41 (2005) 1424–1425.
- [52] S.M. Sondhi, R. Rani, P. Roy, S.K. Agrawal, A.K. Saxena, *Bioorg. Med. Chem. Lett.* 19 (2009) 1534–1538.
- [53] S.M. Sondhi, R. Rani, P. Roy, S.K. Agrawal, A.K. Saxena, *Eur. J. Med. Chem.* 45 (2010) 902–908.
- [54] M.K. Piestrzeniewicz, D. Wilmanska, J. Szemraj, K. Studzian, M.Z. Gniazdowski, *Naturforsch 59c* (2004) 739–748.
- [55] R.E. Mitchell, K.L. Teh, *Org. Biomol. Chem.* 3 (2005) 3540–3543.
- [56] G. Enjun, L. Lei, Z. Mingchang, W. Qiong, *Chin. J. Chem.* 27 (2009) 1285–1290.
- [57] F. Huq, H. Tayyem, J.Q. Yu, P. Beale, K. Fisher, *Med. Chem.* 5 (2009) 372–381.
- [58] B.A.D. Neto, A.A.M. Lapis, *Molecules* 14 (2009) 1725–1746.